A&A 379, L39–L43 (2001)
DOI: 10.1051/0004-6361:20011485

Astronomy & Astrophysics

Possible detection of hard X-ray afterglows of short γ-ray bursts

D. Lazzati[1], E. Ramirez-Ruiz[1], and G. Ghisellini[2]

[1] Institute of Astronomy, University of Cambridge, Madingley Road, CB3 0HA Cambridge, UK
e-mail: enrico@ast.cam.ac.uk
[2] Osservatorio Astronomico di Brera, via Bianchi 46, 23807 Merate, Italy
e-mail: gabriele@merate.mi.astro.it

Received 31 August 2001 / Accepted 10 October 2001

Abstract. We report the discovery of a transient and fading hard X-ray emission in the BATSE lightcurves of a sample of short γ-ray bursts. We have summed each of the four channel BATSE light curves of 76 short bursts to uncover the average overall temporal and spectral evolution of a possible transient signal following the prompt flux. We found an excess emission peaking ∼30 s after the prompt one, detectable for ≈100 s. The soft power-law spectrum and the time-evolution of this transient signal suggest that it is produced by the deceleration of a relativistic expanding source, as predicted by the afterglow model.

Key words. gamma rays: bursts – radiation mechanisms: non-thermal

1. Introduction

Since their discovery in 1973 (Klebesadel et al. 1973), γ-ray bursts (GRBs) have been known predominantly as brief, intense flashes of high-energy radiation, despite intensive searches for transient signals at other wavelengths. Fortunately, the rapid follow-up of *Beppo*SAX (Boella et al. 1997) positions, combined with ground-based observations, has led to the detection of fading emission in X-rays (Costa et al. 1997), optical (van Paradijs et al. 1997) and radio (Frail et al. 1997) wavelengths. These afterglows in turn enabled the measurement of redshifts (Metzger et al. 1997), firmly establishing that GRBs are the most luminous known events in the Universe and involve the highest source expansion velocities (Piran 1999; Mészáros 2001).

Already in the early times of BATSE observations, it was noted that the bursts can be divided into at least two classes based on their duration and spectral hardness (Kouveliotou et al. 1993). The two subclasses are usually classified as short and long GRBs, since the difference in duration is more evident than in hardness (see Fig. 1). The long bursts, with a duration[1] $T_{90} \geq 2$ s, are usually characterized by softer spectra with respect to the long ones. It is also generally believed that the progenitor of the two classes of bursts may be different (Lattimer & Schramm 1976; Rees 1999): hypernovae (Paczynski 1998) or collapsars (MacFadyen & Woosley 1999) for long bursts and mergers of compact binary systems (Eichler et al. 1989) for short ones.

The detection of afterglows that follow systematically long bursts has been a major breakthrough in GRB science (van Paradijs et al. 2000). Unfortunately no observation of this kind was possible for short bursts. Our physical understanding of their properties was therefore put in abeyance, waiting for a new satellite better suited for their prompt localization (Vanderspek et al. 1999).

In this letter we show that afterglow emission characterizes also the class of short bursts. In a comparative analysis of the BATSE lightcurves of short bursts (see Sect. 2), we detect a hard X-ray fading signal following the prompt emission with a delay of ∼30 s. The spectral and temporal behavior of this emission is consistent with the one produced by a decelerating blast wave (see Sect. 3), providing a direct confirmation of relativistic source expansion (Piran 1999).

2. Data analysis

The detection of slowly variable emission in BATSE lightcurves is a non trivial issue, since BATSE is a non-imaging instrument and background subtraction can not be easily performed. We selected from the BATSE GRB catalog[2] (Paciesas et al. 1999) a sample of short duration ($T_{90} \leq 1$ s), high signal-to-noise ratio, GRB lightcurves with continuous data from ∼120 s before the trigger to ∼230 s afterwards. We aligned all the lightcurves to a common time reference in which the burst (binned to a

Send offprint requests to: D. Lazzati,
e-mail: lazzati@ast.cam.ac.uk

[1] T_{90} is the time interval in which the observed fluence rises from 5% to 95% of the total.

[2] The most recent version of the catalog can be found at: http://www.batse.msfc.nasa.gov/batse/grb/catalog/

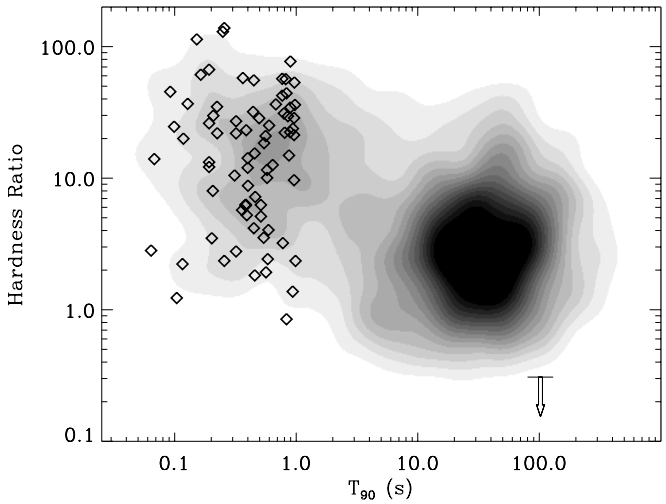

Fig. 1. The hardness-ratio vs. T_{90} space distribution of BATSE GRBs. The hardness ratio is computed as the ratio of the fluence of each burst in the energy channels 3 and 4 divided by the fluence in the channels 1 and 2. Diamonds show the position in the diagram of the 76 short bursts selected for the search of an hard X-ray afterglow. The arrow in the lower right corner marks the upper limit on the hardness ratio of the afterglow emission discussed in this paper.

time resolution of 64 ms) peaked at $t = 0$ and we binned the lightcurves in time by a factor 250, giving a time resolution of 16.0 s. The time bin $[-8 < t < 8$ s] containing the prompt emission was removed and the remaining background modelled with a 4th degree polynomial. The bursts in which this fit yielded a reduced χ^2 larger than 2 in at least one of the four channels were discarded. Note that we did not subtract this best fit background curve from the data. This procedure was used only to reject lightcurves with very rapid and unpredictable background fluctuations and is based on the assumption that the excess burst or afterglow emission is not detectable in a single lightcurve. The position of the selected bursts in the hardness duration plane is shown with diamonds in Fig. 1. This procedure yielded a final sample of 76 lightcurves, characterized by an average duration $\langle T_{90}\rangle = 0.44$ s and fluence $\langle \mathcal{F}\rangle = 2.6 \times 10^{-6}$ erg cm^{-2}.

To search for excess emission following the prompt burst, we added the selected binned lightcurves in the four channels independently. The resulting lightcurves are shown in the upper panels of Fig. 2 by the solid points. Error bars are computed by propagating the Poisson uncertainties of the individual lightcurves.

The lightcurves in the third and fourth channels can be successfully fitted with polynomials. The third (110–325 keV) and fourth (>325 keV) channel lightcurves can be fitted with a quadratic model, yielding χ^2/d.o.f. = 17/18 and χ^2/d.o.f. = 18.5/17 respectively. In the first two channels, a polynomial model alone does not give a good description of the data. In the first (25–60 keV) channel, a cubic fit yields χ^2/d.o.f. = 42/16, while in the second (60–110 keV) we obtain χ^2/d.o.f. = 26/16. A more accurate modelling of the first two channels lightcurves can be achieved by allowing for an afterglow emission following the prompt burst. We model the afterglow lightcurve with a smoothly joined broken power-law function:

$$L_{\rm A}(t) = \frac{3\,L_{\rm A}}{\left(\frac{t_{\rm A}}{t}\right)^2 + \frac{2\,t}{t_{\rm A}}}; \quad t > 0 \qquad (1)$$

which rises as t^2 up to a maximum $L_{\rm A}$ that is reached at time $t_{\rm A}$ and then decays as t^{-1} (Sari 1997). Adding this afterglow component to the fit, we obtain χ^2/d.o.f. = 28.5/16 and 14.7/16 in the first and second channels, respectively[3]. The χ^2 variation, according to the F-test, is significant to the $\sim 3.5\sigma$ level in both channels. The fact that the fit in the first channel is only marginally acceptable should not surprise. This is because the excess is due to many afterglow components peaking at different times, and has therefore a more "symmetric" shape than Eq. (1). A fully acceptable fit can be obtained with a different shape of the excess, but we used the afterglow function for simplicity. By adding together the first two channels, the afterglow component is significant at the 4.2σ level. The results of the fit are reported in Table 1.

Table 1. Fit results. Quoted errors at 90% levels, upper limits at 3σ level.

	E (keV)	$L_{\rm A}$ (cts s^{-1})	$t_{\rm A}$ (s)
Channel #1	[25–60]	8.9 ± 2.6	40 ± 16
Channel #2	[60–110]	7.1 ± 2.4	30^{+16}_{-10}
Channel #1+2	[25–110]	16 ± 3.5	33.5^{+24}_{-15}
Channel #3	[110–325]	<6.6	33.5 (fixed)
Channel #4	>325	<6.0	33.5 (fixed)

A similar attempt to detect long timescale emission in BATSE lightcurves was performed by Connaughton (2000). In that paper excess emission after the main burst was detected in long GRBs, but no signal was detected for short GRBs. The main difference with respect to the present work is that Connaughton (2000) performed the analysis on the total lightcurves (summed over the four channels) and that the short bursts selection was based only on the duration ($T_{90} < 2$ s) and not on the signal-to-noise ratio. In addition, Connaughton (2000) performed a burst by burst background subtraction measuring the background of the single events by averaging the signal of the 15 *Compton*GRO orbits before and after the burst. Since these data are not available in the BATSE public archive, we cannot perform the same analysis and check our results with this method. However, by adding the four channel data, the significance of our detection drops to less than 2σ while, relaxing the constraint on the signal-to-noise ratio in the sample selection, we detect no afterglow in the sum of the resulting 280 lightcurves sample. We believe that a check of the robustness of this detection against the background subtraction technique of Connaughton (2000) would yield interesting results.

[3] This lightcurve is appropriate for the bolometric afterglow luminosity and it is only an approximation for the flux integrated in a spectral band.

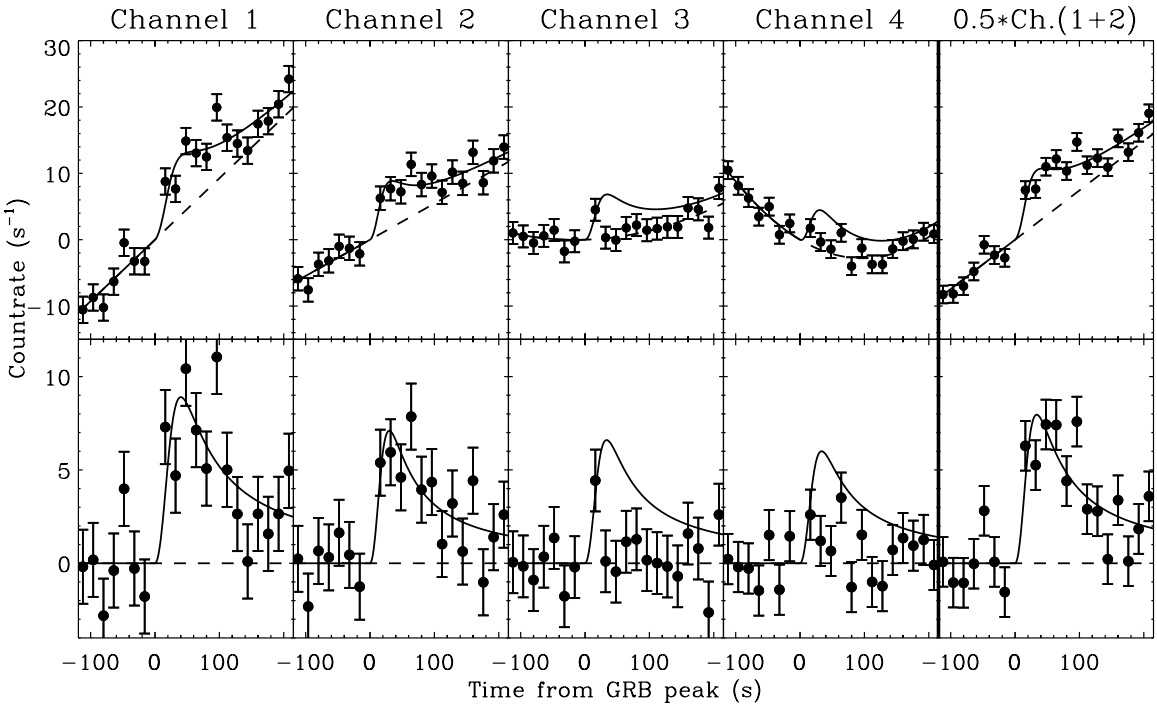

Fig. 2. Overall lightcurves in the 4 BATSE channels (from left to right) of the sample of short bursts (see text). The rightmost panels show the average signal in the first and second channels. The time interval of the burst emission has been excluded. The upper panels show the lightcurves without background subtraction (a constant has been subtracted in all panels for viewing purposes in order to have zero counts at $t = 0$). The solid line is the best fit background plus afterglow model (in the channel 3 and 4 panels the 3σ upper limit afterglow is shown). The dashed line shows the background contribution in all channels. The lower panels show the same data and fit after background subtraction.

2.1. Further statistical tests

To test the robustness of the result we reanalyzed the data with the following procedure. We fit the background of each lightcurve in the time intervals $-120 < t < -8$ s and $\tilde{t} < t < 230$ s with a 4th degree polynomial with $50 < \tilde{t} < 120$ s. We then subtracted the best fit background from each lightcurve at all times. We finally averaged the residuals in the four BATSE channels. Even though the actual shape of the residuals depends on the value of $\tilde{t}$, in all cases we found excesses in the first two BATSE channels and a null results in the third and fourth channels. We checked for the possibility of a single burst lightcurve dominating this detection by recursively subtracting one lightcurve. Performing the same analysis the statistical significances given above were not altered. As a further test we applied the same analysis to a sample of low signal-to-noise short GRBs and to a sample of blank BATSE background lightcurves[4]. In both cases we obtained a null result.

In all the analysis and tests described above, we assumed that the uncertainty in the countrates are purely Poissonian. To check the correctness of this assumption we computed the errors of the mean lightcurve from the dispersion of the sample and not by propagation of the statistical error of each curve. Even though the actual result depends slightly on the degree of the polynomial function used to detrend each individual lightcurve, we find that the errors shown in Fig. 2 are increased by less than 10% and the significance of the feature is only marginally modified.

We finally explored the possibility that the detected signal is residual emission from the burst by fitting a background plus a single power-law to the data. These fits did not significantly decrease the χ^2 with respect to background alone (see also Sect. 3 for the spectral analysis).

3. Discussion

In order to understand whether the excess is residual prompt burst emission or afterglow emission, we computed its four channel spectrum. To convert BATSE count rates to fluxes, we computed an average response matrix for our burst sample by averaging the matrices of single bursts obtained from the `discsc_bfits` and `discsc_drm` datasets. The resulting spectrum is shown in Fig. 3. The dark points show the spectrum at $t = 30$ s (the peak of the afterglow in the second BATSE channel), which is consistent with a single power-law $F(\nu) \propto \nu^{-1}$ (black dashed line). Grey points show the time integrated spectrum (fluences has been measured with a growth curve technique), consistent with a steeper power-law $F(\nu) \propto \nu^{-1.5}$ (grey dashed line). These power-law spectra are much softer than any

[4] These lightcurves were obtained extracting the data in the interval $50 < t < 400$ ($t = 0$ is set by the GRB trigger) from a sample of 62 short low signal-to-noise GRB lightcurves.

observed burst spectrum (independent of their duration). The upper limit of the hardness ratio is shown in Fig. 1 with an arrow in the lower right corner. This spectral diversity, together with the fact that a single power-law does not fit the data, suggest that the emission is not due to a tail of burst emission but more likely to an early hard X-ray afterglow. This also confirms earlier predictions that the mechanism responsible for the afterglow emission is different from that of the prompt radiation (e.g. Piran 1999).

Hard X-ray prompt afterglows have been detected for the long bursts GRB 920723 (Burenin et al. 1999) observed by GRANAT/SIGMA and GRB 980923 (Giblin et al. 1999) observed with BATSE. In both these events a power-law decaying tail was observed at the end of the prompt emission associated with a spectral transition. The derived $t_{\rm A}$ in these bursts was ∼6 s and 9.6 s, respectively. The observed peak time of bolometric afterglow emission is given by (Sari 1997):

$$t_{\rm A} = 93.6\,(1+z)\left(\frac{E}{10^{52}\ {\rm erg}}\right)^{1/3}\left(\frac{\Gamma}{100}\right)^{-8/3} n^{-1/3}\ {\rm s} \quad (2)$$

where z is the redshift, E is the isotropic equivalent kinetic energy of the fireball, Γ is the asymptotic Lorentz factor and n the baryon number density of the external medium.

The shorter $t_{\rm A}$ detected in long bursts may hence reflect a higher Lorentz factor Γ or external density n in long GRBs with respect to short ones (see Eq. (2)). A smaller external density would indeed be required if short bursts are associated to mergers of compact objects (Eichler et al. 1989). Less likely, given the constraints on the $\langle V/V_{\rm max}\rangle$ of the two classes, the longer peak time may be due to a higher redshift or a larger kinetic energy of the fireball (Lee & Petrosian 1997; Schmidt 2001). On the other hand, the optical flash observed in the long burst GRB990123 (Akerlof et al. 1999), had a peak time $t_{\rm A} \sim 40$ s, showing that a dispersion of the Γ and n parameters is present within a single burst class.

The detected peak flux of $\sim 10^{-11}$ erg cm^{-2} s^{-1} keV^{-1} (∼0.004 mJy) at 50 keV can be compared with sparse measurements of short/intermediate GRBs. Measurements at comparable times (10−100 s) have been possible only with robotic optical telescopes for three short bursts detected by BATSE (Kehoe et al. 2001). These measurements yielded upper limits of ∼5 mJy in unfiltered CCD images. Assuming a flat $F(\nu) \propto \nu^0$ spectrum this upper limits are much brighter than our detected average afterglow. An optical and radio afterglow was detected and intensely observed for the intermediate duration ($T_{90} \sim 2$ s) burst GRB000301C (Masetti et al. 2000). The multiwavelength afterglow of this burst can be fitted by an external shock model (Panaitescu & Kumar 2001b). The extrapolated flux at 50 keV ∼ 50 s after the burst event is ∼0.01 mJy, in good agreement with our detection.

Another interesting comparison can be made with the early afterglow of long GRBs. Connaughton (2000) finds that on average the BATSE countrate is ∼150 cts s^{-1} at $t = 50$ s after the main event. In our short GRB sample, the countrate at the same time is ∼15 cts s^{-1}. Since the luminosity of the average early X-ray afterglow is representative of the total isotropic energy of the fireball (Kumar 2000), we can conclude that the isotropic equivalent energy of the short bursts is on average ten times smaller than that of the long ones (or that their true energy is the same, but the jet opening angle is three times larger). Indeed, the γ-ray fluence of long bursts is on average ten times larger than that of short bursts.

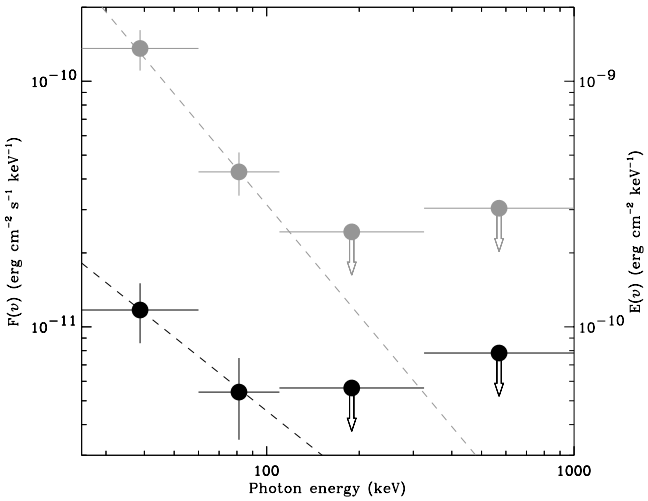

Fig. 3. Spectrum of the peak afterglow emission. Black dots (and left vertical axis) show the spectrum at $t = 30$ s. Gray dots (right vertical axis) show the time integrated spectrum as obtained from the four BATSE channel counts. Error bars are for 90% uncertainties, while arrows are 3σ upper limits.

In the case of short bursts, the analysis of the afterglow emission is made easier by the lack of superposition with the prompt burst flux. For this reason the time and luminosity of the afterglow peak can be directly measured while in long bursts it had to be inferred from the shape of the decay law at longer times (Burenin et al. 1999; Giblin et al. 1999). In our case, however, the lightcurve in Fig. 2 is the result of the sum of many afterglow lightcurves, with different peak times and luminosities. For a given isotropic equivalent energy E, afterglows peaking earlier (with larger Γ) are expected to be brighter and should dominate the composite lightcurve. On the other hand, for a given Lorentz factor Γ, afterglow peaking earlier (with lower E) are dimmer. The fact that the ∼35 s timescale is preserved, suggests that there are only few very energetic bursts with a large bulk Lorentz factor.

In the external shock model, the multiwavelength lightcurve of the afterglow can be calculated (see Panaitescu & Kumar 2000 and references therein), given the properties of the fireball (initial bulk Lorentz factor Γ and isotropic equivalent energy E), the external medium density n and the shock properties (the equipartition parameters $\epsilon_{\rm e}$ and $\epsilon_{\rm B}$, the slope of the electron power-law distribution p and the γ-ray efficiency η). Some of the parameters in the above set are poorly constrained, like the

equipartition parameters $\epsilon_{\rm B}$ and $\epsilon_{\rm E}$. In the following we will adopt the logarithmically averaged $\langle\epsilon_{\rm B}\rangle = 0.004$ and $\langle\epsilon_{\rm e}\rangle = 0.06$, obtained by Panaitescu & Kumar (2001) by fitting lightcurves and spectra of long GRB afterglows.

The peak in the lightcurve observed at $t \sim 35$ s can be associated either (a) with the beginning of the afterglow (fireball deceleration, see Eq. (2)) or (b) with the transition of the peak of the spectrum in the observed band. In the first case, the peak time coincides with the deceleration time. In the second case, the peak time follows the deceleration time with some delay and the peak of the spectrum must be at ~ 50 keV at $t \sim 35$ s. These two constraints ($t_{\rm a} < 50$ s and $25 < h\nu_{\rm peak} < 110$ keV) can be simultaneously satisfied only for $\Gamma > 200$ and $\epsilon_{\rm e} > 0.1$. In addition, the observed spectrum is expected to be either $F(\nu) \propto \nu^{-1/2}$ (fast cooling) or $F(\nu) \propto \nu^{-(p-1)/2}$ (slow cooling, where $p \sim 2.5$ is the index of the power-law distribution of electrons), harder than what is observed.

If the observed peak is instead due to the time of deceleration of the fireball [case (a) above], a consistent solution can be found for the parameter set $z \sim 0.4$, $n \sim 10^{-1}$ cm^{-3}, $\Gamma = 100$, $E \sim 5 \times 10^{51}$ erg and $\eta = 0.2$. An electron distribution $n(\gamma) \propto \gamma^{-2.5}$ was also assumed, consistent with the spectrum of Fig. 3 (in this regime the spectral slope is given by $F(\nu) \propto \nu^{-p/2}$). The data are hence consistent with the possibility that short bursts have a similar energy budget to the long ones, but with a 3−10 times larger jet opening angle. On this basis, it is also possible to predict the flux and fluence at the time at which follow-up observations are typically performed. In X-rays, usually observed at $t = 8$ h, the predicted flux is $F_{[2-10]\rm keV} \sim 3 \times 10^{-13}$ erg cm^{-2} s^{-1}. In the optical, at $t = 12$ h, we predict a magnitude $R \sim 22$. Both these fluxes should be within the detection capabilities of present instrumentation (see also Panaitescu et al. 2001).

It is interesting also to explore whether a consistent solution can be found for very small redshifts, or even for short bursts exploding in our own galaxy. This is plausible for the following parameter set: $d = 100$ kpc; $n \sim 10^{-4}$ cm^{-3}; $\Gamma = 20$ and $E \sim 2 \times 10^{43}$ erg. However in this case the typical frequency emitted by the injected electrons is in the optical band (Panaitescu & Kumar 2000) and the solution is only valid if the power-law of accelerated electrons extends for more than four orders of magnitude. In addition, the analysis of the number counts of short and long bursts suggest a similar average redshift for the two populations (Schmidt 2001).

We must also remain aware of other possibilities. For instance, we may be wrong in assuming that the central object goes dormant after producing the initial explosion. A sudden burst followed by a slowly decaying energy input could arise if the newly formed black hole slowly swallows the orbiting torus around it or if the central object becomes a rapidly-spinning pulsar rather than a black hole (Rees 1999). This luminosity may dominate the continuum afterglow at early times before the blast wave decelerates. Under this interpretation, the hard X-ray transient following the prompt emission could be attributed to the central object itself rather than to a standard decelerating blast wave. Contrary to what is observed, this emission should smoothly decay after the main episode, unless this energy is converted into a relativistic outflow which is in turn converted to radiation at a larger radius.

Acknowledgements. We thank the anonymous referee for his carefully and constructive reading of the manuscript. We thank Luigi Stella for many stimulating comments and suggestions and Martin J. Rees, Sergio Campana, William Lee and Elena Rossi for useful conversations.

References

Akerlof, C., Balsano, R., Barthelemy, S., et al. 1999, Nature, 398, 400
Boella, G., Butler, R. C., Perola, G. C., et al. 1997, A&AS, 122, 299
Burenin, R. A., Vikhlinin, A. A., Gilfanov, M. R., et al. 1999, A&A, 344, L53
Connaughton, V. 2000, in Proceedings of Gamma-ray bursts: 5th Huntsville Symposium, Huntsville, AL, Oct. 1999, ed. R. M. Kippen, R. S. Mallozzi, & G. J. Fishman
Costa, E., Frontera, F., Heise, J., et al. 1997, Nature, 387, 783
Eichler, D., Livio, M., Piran, T., & Schramm, D. N. 1989, Nature, 340, 126
Frail, D A., Kulkarni, S. R., Nicastro, S. R., Feroci, M., & Taylor, G. B. 1997, Nature, 389, 261
Giblin, T., van Paradijs, J., Kouveliotou, C., et al. 1999, ApJ, 524, L47
Kehoe, R., Akerlof, C., Balsano, R., et al. 2001, ApJ, 554, L159
Klebesadel, R. W., Strong, I. B., & Olson, R. A. 1973, ApJ, 182, L85
Kouveliotou, C., Meegan, C. A., Fishman, G. J., et al. 1993, ApJ, 413, L101
Kumar, P. 2000, ApJ, 538, L125
Lattimer, J. M., & Schramm, D. N. 1976, ApJ, 210, 549
Lee, T. T., & Petrosian, V. 1997, ApJ, 474, 37
MacFadyen, A. I., & Woosley, S. E. 1999, ApJ, 524, 262
Masetti, N., Bartolini, C, Bernabei, S., et al. 2000, A&A, 359, L23
Mészáros, P. 2001, Science, 291, 79
Metzger, M. R., Djorgovski, S. G., Kulkarni, S. R., et al. 1997, Nature, 387, 878
Paciesas, W. S., Meegan, C. A., Pendleton, G. N., et al. 1999, ApJS, 122, 465
Paczynski, B. 1998, ApJ, 494, L45
Panaitescu, A., & Kumar, P. 2000, ApJ, 543, 66
Panaitescu, A., & Kumar, P. 2001, ApJ, 554, 667
Panaitescu, A., & Kumar, P. 2001, ApJ, submitted [astro-ph/0109124]
Panaitescu, A., Kumar, P., & Narayan, R. 2001, ApJ, submitted [astro-ph/0108132]
Piran, T. 1999, Phys. Rep., 314, 575
Rees, M. J. 1999, A&AS, 138, 491
Sari, R. 1997, ApJ, 489, L37
Schmidt, M. 2001, ApJL, in press [astro-ph/0108459]
Vanderspek, R., Villaseñor, J., Doty, J., et al. 1999, A&AS, 138, 565
van Paradijs, J. P., Groot, P. J., Galama, T., et al. 1997, Nature, 386, 686
van Paradijs, J., Kouveliotou, C., & Wijers, R. A. M. J. 2000, ARA&A, 38, 379